Brazilian Journal of Geophysics (2023) 40(Suppl. 1): 141-159
Brazilian Geophysical Society
ISSN 2764-8044
DOI: 10.22564/brjg.v40i5.2151

IONOSPHERIC SCINTILLATION CHARACTERISTICS AND THEIR EFFECTS OVER GNSS SIGNAL AND POSITION AND NAVIGATION SYSTEMS AT BRAZILIAN REGION

Eurico R. de Paula [1*], Alison de Oliveira Moraes [2] and João Francisco Galera Monico [3]

[1] Instituto Nacional de Pesquisas Espaciais - INPE, São José dos Campos, SP, Brazil
[2] IAE- Instituto de Aeronáutica e Espaço - DCTA, São José dos Campos, SP, Brazil
[3] Universidade Estadual Paulista Júlio de Mesquita Filho, Presidente Prudente, SP, Brazil

*Corresponding author e-mail: eurico.paula@inpe.br

ABSTRACT. The ionosphere is an ionized layer extending from about 50 km to 1,000 km of altitude. When an electromagnetic signal crosses this layer it suffers a delay in its group velocity and an advance in its phase velocity. The ionosphere is very dynamic and after the sunset its F region equatorial bottomside is lifted up by the intensified eastward electric field, giving origin to an steep plasma gradient. This configurates an unstable condition with higher density plasma standing over lower density one. Seeding mechanisms (Abdu et al., 2015) like gravity waves, if exist at this region, create favorable conditions for the Rayleigh-Taylor interchange plasma instability to develop. This instability pushes rarified plasma upward giving origin to large regions named Equatorial Plasma Bubbles (EPB) that rise at equatorial regions and map to low latitudes along the magnetic field lines and can reach continental extension. Through cascating process, small scale irregularities (cm to km) are generated inside the EPBs. Due to refractive effects, amplitude and phase scintillations are generated in the signal crossing these irregularities. Transionospheric signals used in telecommunication links and in the GNSS applications are severely affected during ionospheric scintillations. In this work we will present the ionospheric scintillation morphology over Brazilian longitudinal sector, its effects over positioning and navigation systems and the existing methodology to mitigate them.

Keywords: ionosphere physics, ionospheric scintillation, GNSS, GBAS and SBAS, threat model.

INTRODUCTION

The ionospheric scintillation due to plasma irregularities presents a large day-to-day variability and suffer the influence of the local time, season, solar flux, geomagnetic location and geomagnetic activity conditions (Moraes et al., 2017; Muella et al., 2017; Abdu, 2019). The relative direction of the GNSS signal in relation to the bubble direction is an important factor that should be accounted for (Moraes et al., 2017). The signal scintillation causes GNSS receiver signal loss of lock and cycle slips due to amplitude fades and fast phase variations (Doherty et al., 2003), causing degradation of accuracy (Kintner et al., 2001), availability and integrity of this system. In Brazil degradation of precise agriculture, positioning of petroleum platforms in deep ocean and in aerial navigation systems that uses GNSS signal and their augmentation systems like the SBAS (Satellite Based Augmentation System) and the GBAS (Ground Based Augmentation System) (Sousasantos, et al., 2021; Marini-Pereira, et al., 2021), as well as problems in the SAR (Synthetic Aperture Radar) (Sato et al., 2021) and in the telecommunication systems have been reported during scintillation events. So it is very important to understand the plasma irregularity seeding and evolution mechanisms and also the morphological behavior of the scintillation to try to forecast its occurrence and to mitigate its effects over the systems that use transionospheric signal. The plasma irregularity studies are performed using data mainly

from ionospheric sounders based on the ground or onboard of satellites and using sophisticated simulation models (Yokoyama, 2017). In Brazil, the first scintillation monitor that is a receiver specially prepared to measure the GNSS signal at a high rate (50 to 100 Hz) was installed in 1997 and nowadays there are many scintillation monitor arrays in operation (de Paula et al., 2023). Many of these arrays have the capability to measure scintillation in almost real time (RT) and to provide RT maps, which is a valuable tool for users of GNSS positioning and navigation systems. The large-scale bubble signatures can be displayed using Total Electron Density (TEC) maps (Takahashi et al., 2016; de Oliveira et al., 2020). Many others ionospheric sounders like VHF radar (de Paula and Hysell, 2004), Digisondes, VHF spaced receivers and all-sky imagers complement the scintillation data from GNSS receivers. One historical description of the scintillation and bubble measurements over the Brazilian region is available in de Paula et al. (2021a).

Besides being generated at the magnetic equator, the plasma irregularities can also be locally generated at regions with the presence of large electron density gradients like around the crests of the Equatorial Ionization Anomaly (EIA) that is located around 15º (magnetic latitude) north and south (Muella et al., 2010). One good parameter to represent the ionospheric ionization is the TEC that can be available from the large IBGE/RBMC array in the Brazilian territory. The scintillation monitors cited above also provide TEC. The electron density gradients can be detected by the TEC gradients and from this parameter it is also possible to calculate the Rate of TEC Index (ROTI), which is a good proxy for plasma irregularities and consequently to the ionospheric scintillation. It is worth to mention that the scintillation amplitude is larger where the background ionization (TEC) is large such as around the crests of the EIA. In the next section we describe the S_4 and σ_φ index calculations used to represent the amplitude and phase scintillation respectively and their effects over the GNSS signals L1, L2C and L5. Then, in the following one, it is described the GNSS scintillation morphology, the scintillation effects on the augmentation systems (SBAS, GBAS) and on the positioning and navigation systems including the Real Time Kimematics (RTK). After, in another section, we point out some existing efforts to mitigate the scintillation effects on the systems that use GNSS signal and the final section presents the conclusions.

GNSS SIGNAL AMPLITUDE S4 AND PHASE Σ_Φ SCINTILLATION INDEXES AND SCINTILLATION EFFECTS OVER THIS SIGNAL

S4 and σ_φ calculation

The most used index to represent the amplitude scintillation is the S_4 index which is normally computed according to Van Dierendonck et al., (1993):

$$S_4 = \sqrt{\frac{\langle I^2 \rangle - \langle I \rangle^2}{\langle I \rangle^2}} \qquad (1)$$

where $I=A^2 = I_c^2 + Q_c^2$ is the signal intensity; A is the amplitude of the received signal; I_c and Q_c are the signal intensity in-phase and quadrature components respectively measured in a rate of 50 to 100 Hz; and < > is the ensemble average. It is usual to calculate S_4 at each one minute. So the S_4 index is the standard deviation of signal intensity divided by the mean value of intensity.

The phase scintillation index σ_φ is calculated using the equation (Van Dierendonck et al., 1993):

$$\sigma_\phi = \sqrt{\langle \phi^2 \rangle - \langle \phi \rangle^2} \qquad (2)$$

where ϕ is the unwrapped and detrended carrier phase.

More detailed S_4 and σ_φ calculations are described in de Paula et al. (2021b).

Scintillation effects over the GNSS signal

Figure 1 presents one example of GPS L1 signal amplitude scintillation event (upper panel) and the S_4 index calculated for the same time interval (lower panel), where a good correlation between them can be observed. This example refers to satellite PRN 16 on the night of November 22, 2014, recorded on a scintillation monitor in São José dos Campos, Brazil. It can be seen that as S_4 increases the more intense are the fluctuations in the received signal strength. An interesting analysis about the scintillation error at São José dos Campos, Brazil, for the combination of different GPS signals and frequencies, during the solar maxima 24, can be found in Sousa et al (2022).

It is important to mention that the S_4 index alone does not represent the scintillation severity.

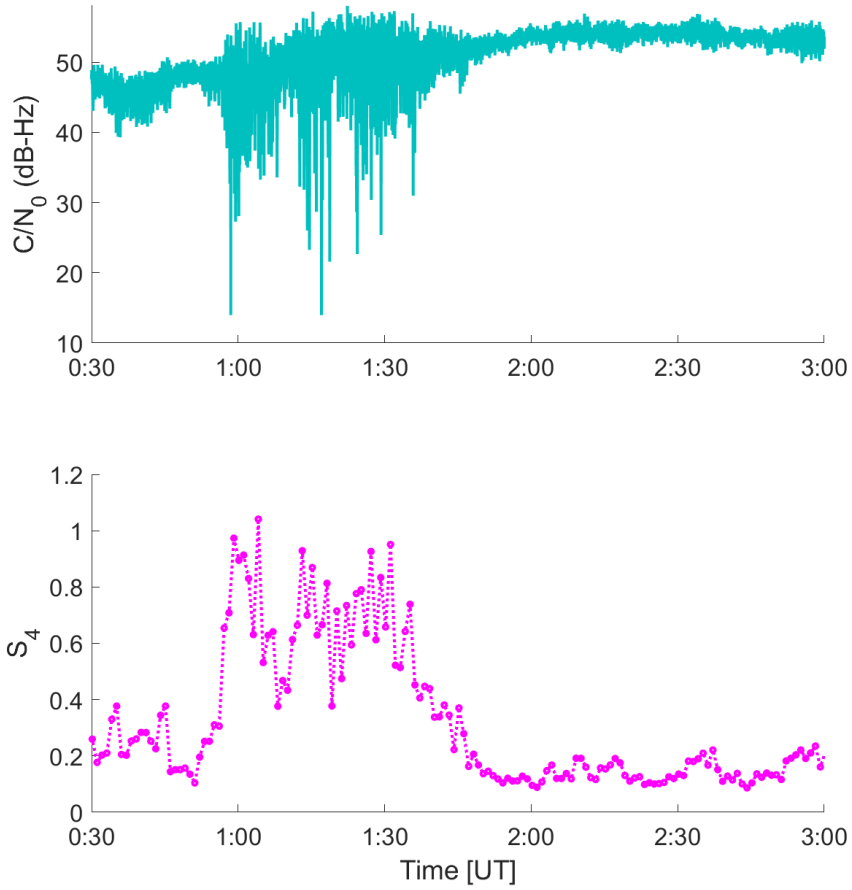

Figure 1: GPS amplitude signal scintillation and the correspondent S_4 index for November 22, 2014, at the site of São José dos Campos (source: the authors).

The decorrelation time parameter τ_0, that is the time lag at which the autocorrelation function falls e^{-1} from its maximum (zero lag) value, may be also considered for. Figure 2 presents the amplitude scintillation for almost the same S_4 value (~0.8) but different 4 values of τ_0 and it can be clearly observed different amplitude scintillation patterns with the fading rate increasing for smaller values of τ_0. This subject was discussed in details in Carrano and Groves (2010), Moraes et al. (2011) and Portella et al. (2021). Finally, it is worth mentioning that auxiliary parameters for scintillation analysis are not limited only to τ_0. In the works of Moraes et al. (2014, 2018a, 2019) examples of the use of statistical models that can be used to differentiate the profile of scintillation are presented.

The inability of the receiver to track and demodulate the received signal is called loss of lock and this is an effect that occurs when the received signal is not of good quality. When loss of lock occurs, that channel is lost and the total number of satellites used in the positioning decreases. For GNSS positioning the parameter that represents the quality of positioning based on the geometry of the satellites is the GDOP (Geometric Dilution of Precision) (Misra and Enge, 2006). The reduction in the number of available satellites is a critical situation caused by strong scintillation that can deteriorate or even hinder the GNSS operation. Figure 3 shows one example of loss of lock for more than four seconds. So the satellite PRN 29 was not available during this time interval, increasing the GDOP.

With the aim of analyzing the performance of triple GNSS frequencies L1, L2C and L5 during scintillation conditions, Moraes et al. (2017) utilized measurements by one Septentrio PolaRxS triple-frequency (L1, L2C, and L5) receiver operated at São José dos Campos (SJC), Brazil, (23.21°S, 45.95°W, −17.5° dip latitude, declination 21.4°W), a site near the southern crest of the equatorial ionization anomaly (EIA). The analysis used S_4 and σ_φ scintillation data from 19:00 LT to 02:00 LT during 01 November 2014 to 30 March 2015. Figure 4 shows the complementary cumulative distribution for S_4 (a) and σ_φ (b). This figure points out that it is possible to state that the modernized signals L2C and L5 are more susceptible to the effects of the ionospheric scintillation

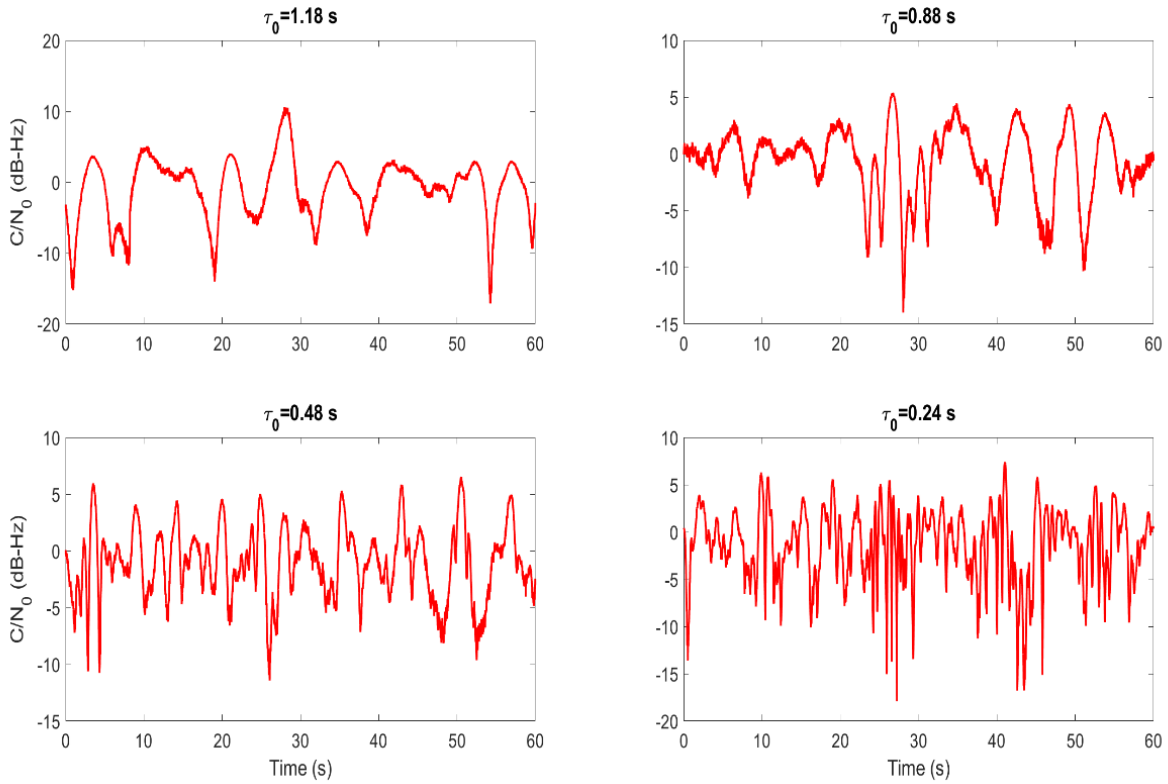

Figure 2: Amplitude scintillation patterns for almost the same S_4 value (S_4 ~ 0.80) but different decorrelation time τ_0 values (source: the authors).

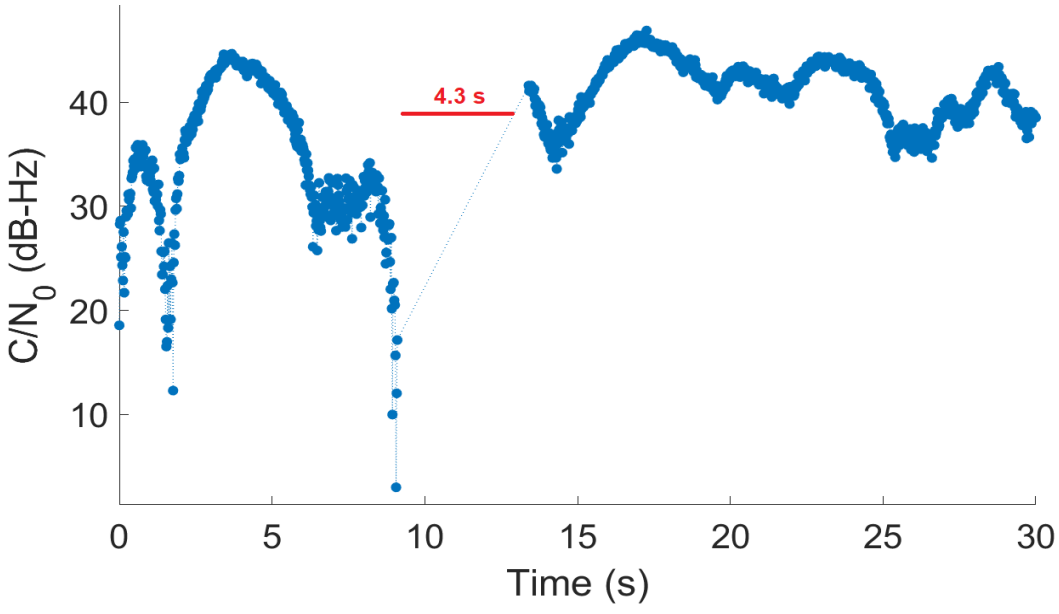

Figure 3: An example of loss of lock with 4.3 s of duration on November 18, 2014, at Presidente Prudente (source: the authors).

in low latitudes. Later on, the work of Salles et al. (2021a,b) deepened this investigation for the same period, but for 4 different locations (Porto Alegre, São José dos Campos, Presidente Prudente and Fortaleza) and they analyzed the fading profile for L1, L2C and L5 signals. The results of these works show that the modernized signals have a higher fading rate, and deeper fades than the legacy L1 signal.

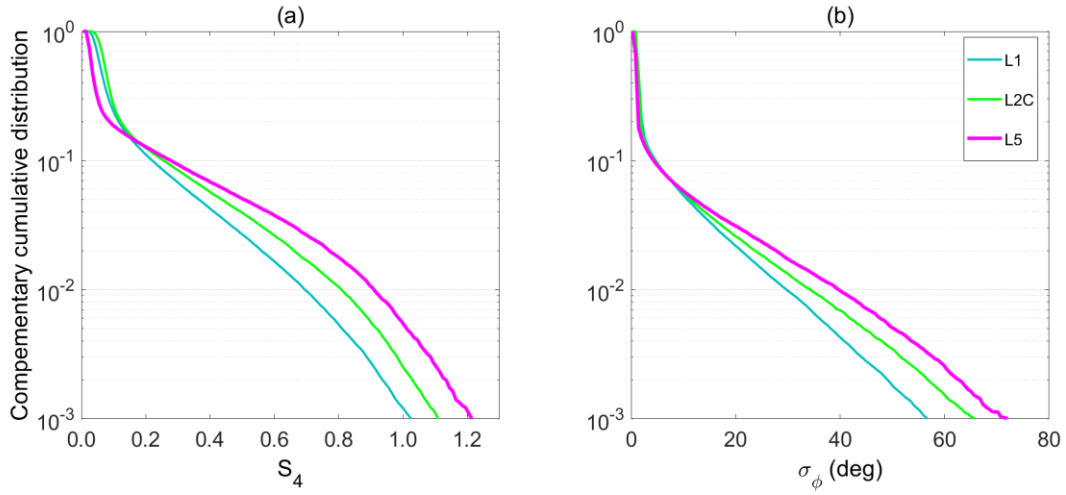

Figure 4: Complementary cumulative distributions of S_4 and σ_φ for the L1, L2C, and L5 signals (source: the authors).

Local Time, Seasonal, Solar Activity, Latitudinal, Longitudinal, Magnetic Activity, And Propagation Path Effects on the Scintillations

The local time, seasonal and solar activity effects over the ionospheric scintillations can be observed in Figure 5. This figure shows the $S_4 > 0.2$ percentage of occurrence from 1998 to 2015, covering the solar cycle 23 and part of 24. It can be observed that the scintillation occurrence at low latitude initiates around 19:30 and lasts up to 01:30 LT for high solar activity (this time interval decreases for low solar activity) and its intensity and percentage of occurrence are higher for higher solar flux. Even though the seasonal behavior is also provided by this figure, a better view of this behavior is shown in Figure 6 which points out that bubbles at Brazilian low latitude (São José dos Campos) starts in September and extends up to March/April (Sobral et al., 2002), having maximum occurrence during summer solstice (November–January).

The scintillation intensity depends of the ionospheric background ionization which is not uniform along the magnetic latitude due to the EIA, being smaller at equatorial regions with crests of ionization north and south around 15° of magnetic latitude. The EIA is intensified during the prereversal hours (18-21 LT). The irregularities are proportional to ΔN, where N is the background ionization and ΔN is the ionization variation. As N increases close to EIA crests ΔN also increases since the ratio ΔN/N remains constant along the magnetic field lines that have a high latitudinal conductivity. Figure 7 shows the S_4 index along the GNSS satellite tracks projected to the ground for November 15, 2022, considering receivers from GNSS NavAer scintillation monitors (Monico et al., 2022). The sites used were Porto Alegre, Presidente Prudente, São José dos Campos, Inconfidentes and Fortaleza, details about those stations can be found in de Paula et al. (2023). So S_4 amplitude increases from magnetic equator where normally they are not larger than about 0.30 to the crest of the EIA where S_4 can reach much large amplitude as 1.40.

Figure 8 also shows the latitudinal S_4 variation from January to March 2000 for 3 sites and for 4 scintillation levels. São José dos Campos is close to the south EIA crest, Cuiabá is located between São José dos Campos and São Luís and São Luís is closer to the magnetic equator.

There are few works about the longitudinal effects over the plasma irregularities at South America. In this longitudinal sector the magnetic declination decreases from east to west. Abdu et al (1998) showed that the spread F (SF – generic term to express ionospheric spread of F layer that occurs during the presence of plasma irregularities) measured by Digisonde was much larger at Cachoeira Paulista (45° W, 22.5° S, -28° dip) when compared to Tucumán (64° W, 27° S, -26° dip), even though these 2 sites have almost the same magnetic latitude. It is worth to mention that the Tucumán magnetic declination was about 3° W while it was 21° W at Cachoeira Paulista for the epoch the data were analyzed. The alignment between the magnetic field lines and the terminator line (day-night) and also the vertical plasma drift at the magnetic equator are important factors that determines the seasonality and the occurrence or not of the irregularities at a specific site. Figure 9 presents the SF behavior at Cachoeira Paulista and Tucumán.

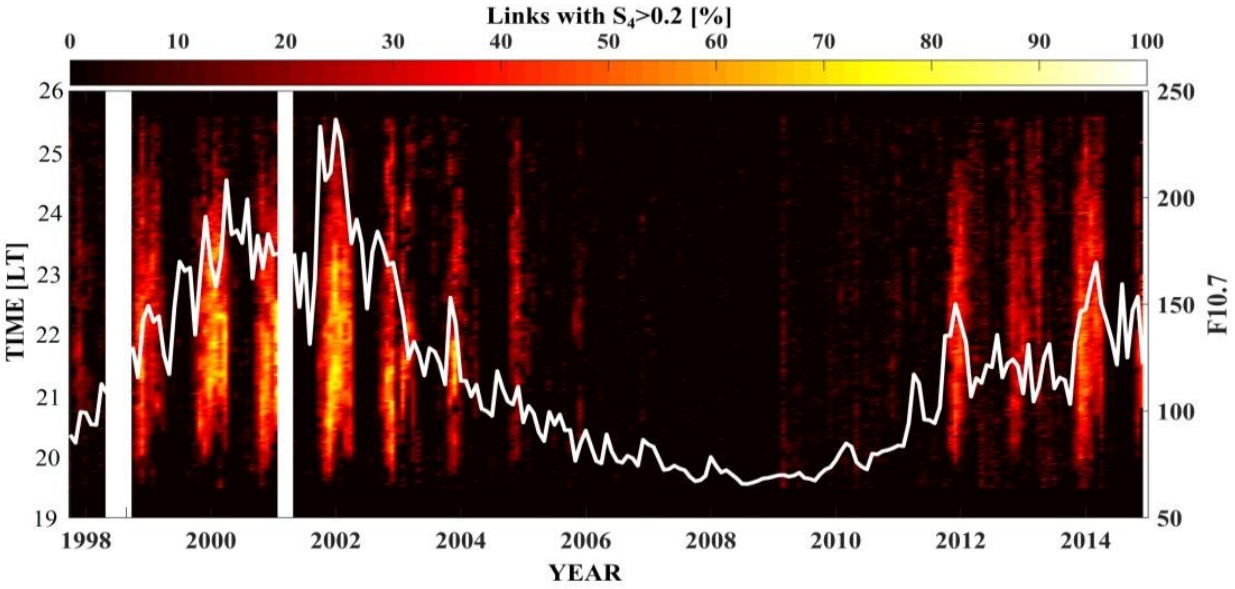

Figure 5: S_4 data from the low-latitude GNSS receiver at Cachoeira Paulista and F10.7 cm solar flux (white continuous curve) from 1998 to 2014 (source: de Paula et al., 2021a).

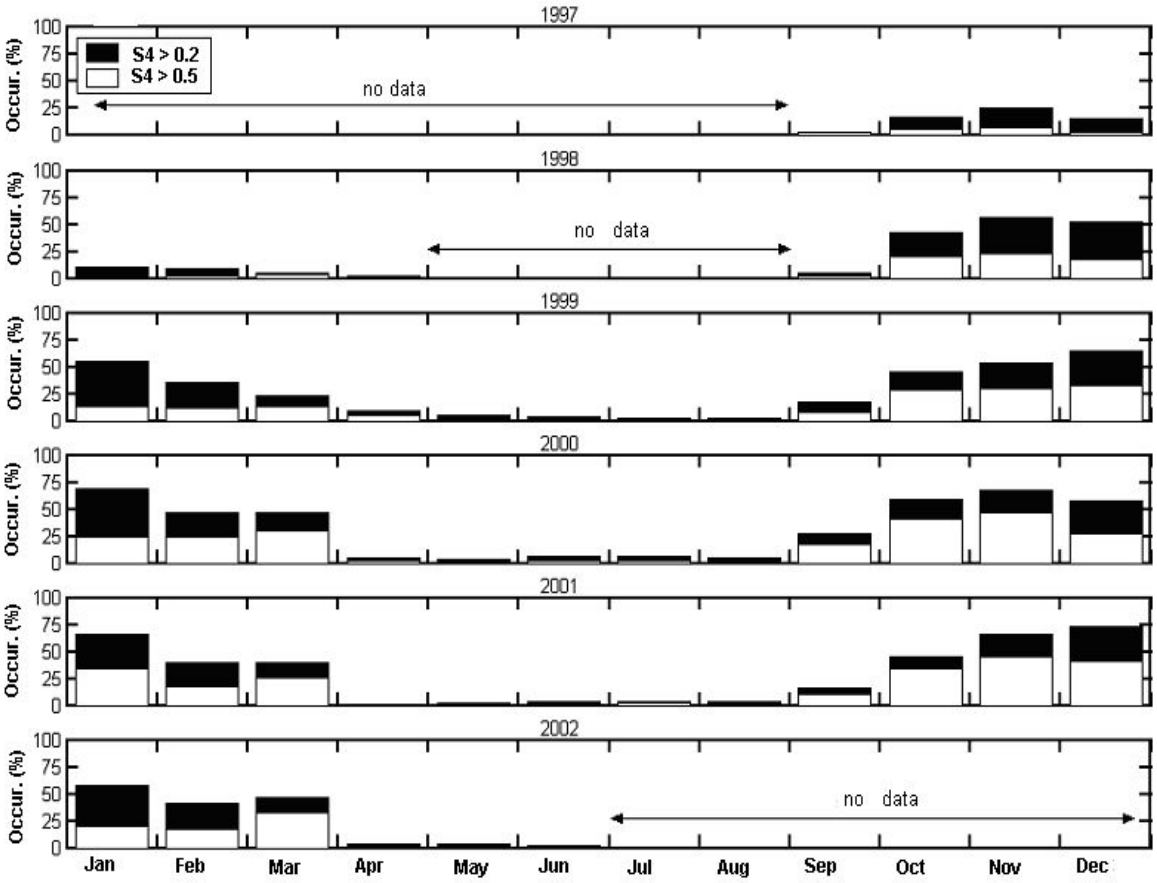

Figure 6: Time percentage between 20 and 01 LT when there was weak and strong ($S_4 > 0.2$) and strong ($S_4 > 0.5$) scintillation occurrence for each month in the period from 1997 to 2002 at São José dos Campos (source: Sobral et al., 2002).

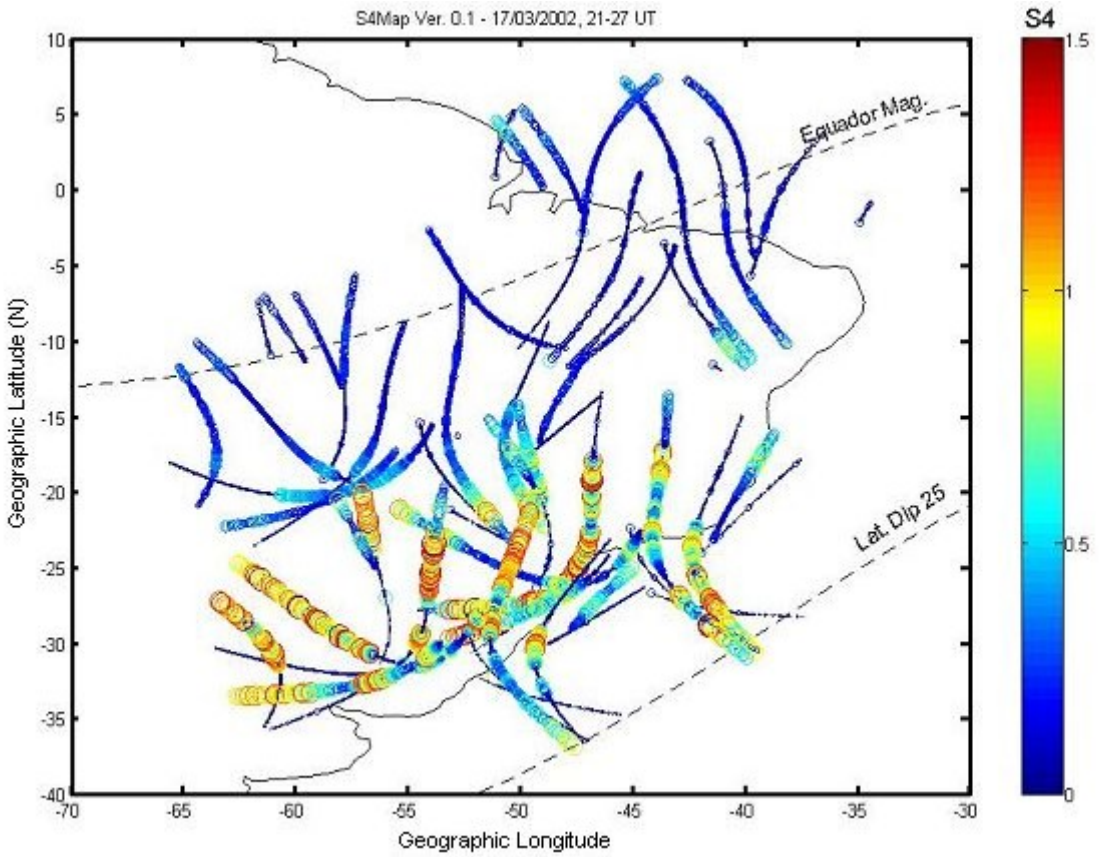

Figure 7: S_4 amplitude along the GNSS satellites for November 15, 2022. Source: the authors.

The magnetic storms have substantial effects over the scintillation. If there is prompt penetration of eastward electric field (PPEF) from magnetosphere into equatorial region during the prereversal hours, the upward plasma drift is intensified (de Paula et al., 2019) and plasma irregularities can be generated even during no scintillation season. Figure 10 presents one example of scintillation triggering during the 10-12 April 2001 strong magnetic storm, when no strong scintillation was expected. Observe that the scintillation was observed only during the night 11/12 at all satellites shown in Figure 9, when the magnetic index Dst reached around -260 nT, which is considered a strong magnetic storm.

During the storm main phase, the high latitude region becomes heated by the auroral intensified currents (Joule effect) and energetic particle precipitations generating a storm time neutral wind blowing initially to the equator direction that generates the disturbance dynamo electric field (DDEF). This electric field is westward during daytime and prereversal hours and inhibits the prereversion plasma drift peak and consequently the generation of plasma irregularities. It takes some hours after the storm main phase for this process to set up one westward electric field at the magnetic equator. Figure 11 shows one example of scintillation inhibition at 8 GNSS satellites during the super strong storm night 20/21 November 2003.

The alignment between the GNSS signal and the magnetic field lines, when the signals are more likely to propagate a longer distance in the turbulent medium created by the bubbles, gives origin to interruptions due to the loss of phase lock (Moraes et al., 2018b), since there are large amplitude fades (canonical) and increased phase scintillations (Sousantos et al., 2022). Figure 12 presents the amplitude scintillation events plotted at the respective IPP (ionospheric piercing point) projections (left panel), the statistical S_4 distribution as function of elevation (middle panel) and the statistics of S_4 as a function of azimuth (right panel) for the periods of 15-30 November 2014 and 04-18 February 2015 for São José dos Campos (23.2° S, 45.9° W, dip latitude: 19.2° S). In the Brazilian region the magnetic declination is around 21° west, so the bubbles generated at the magnetic equator propagates from this direction (NW). According to Figure 12 the most severe scintillations are from satellite tracks aligned with NW magnetic direction, with elevation of about 20° and azimuth between 315° and 360° and the signals from these satellites are prone to have larger losses of lock.

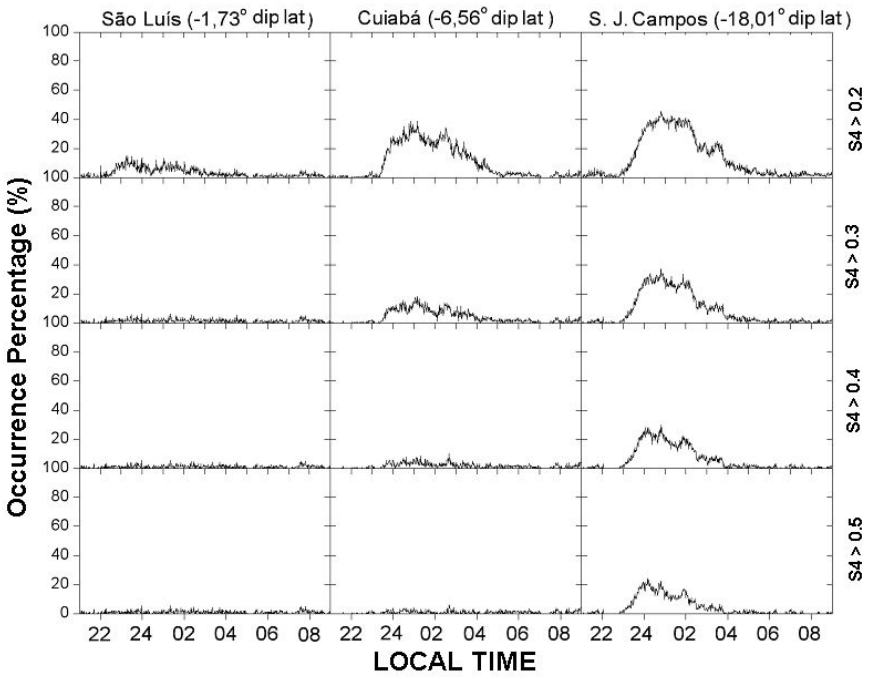

Figure 8: Scintillation occurrence for different intensity levels for 3 GPS sites in the Brazilian Territory from January to March 2000 (source: the authors).

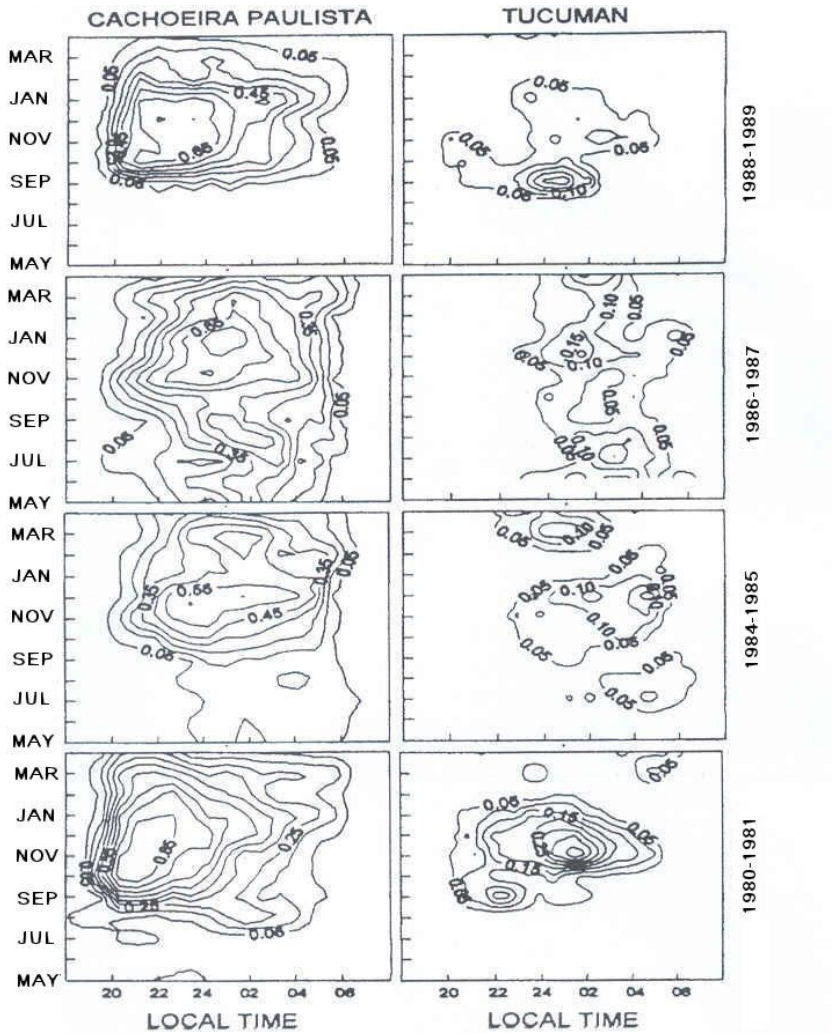

Figure 9: Spread F (SF) at Cachoeira Paulista and Tucumán from 1980 to 1989 (source: Abdu et al., 1998)

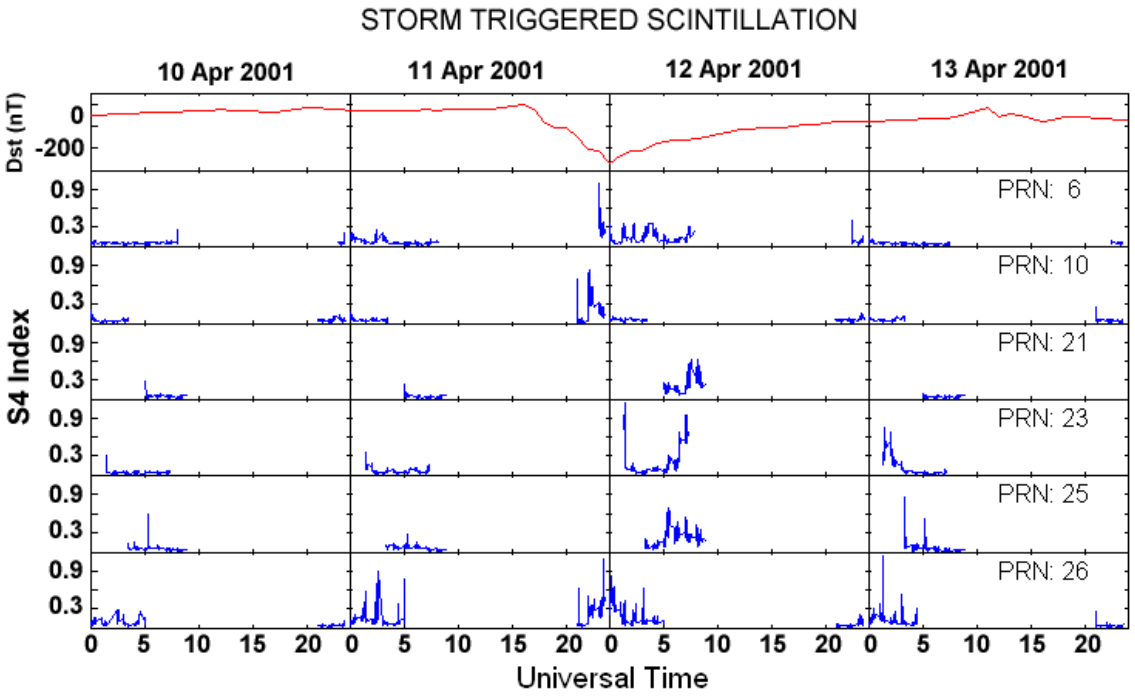

Figure 10: Example of storm scintillation triggering during the night of 11 to 12 of April 2001 under the effect of a strong magnetic storm. In the upper panel it is plotted the Dst index (source: the authors).

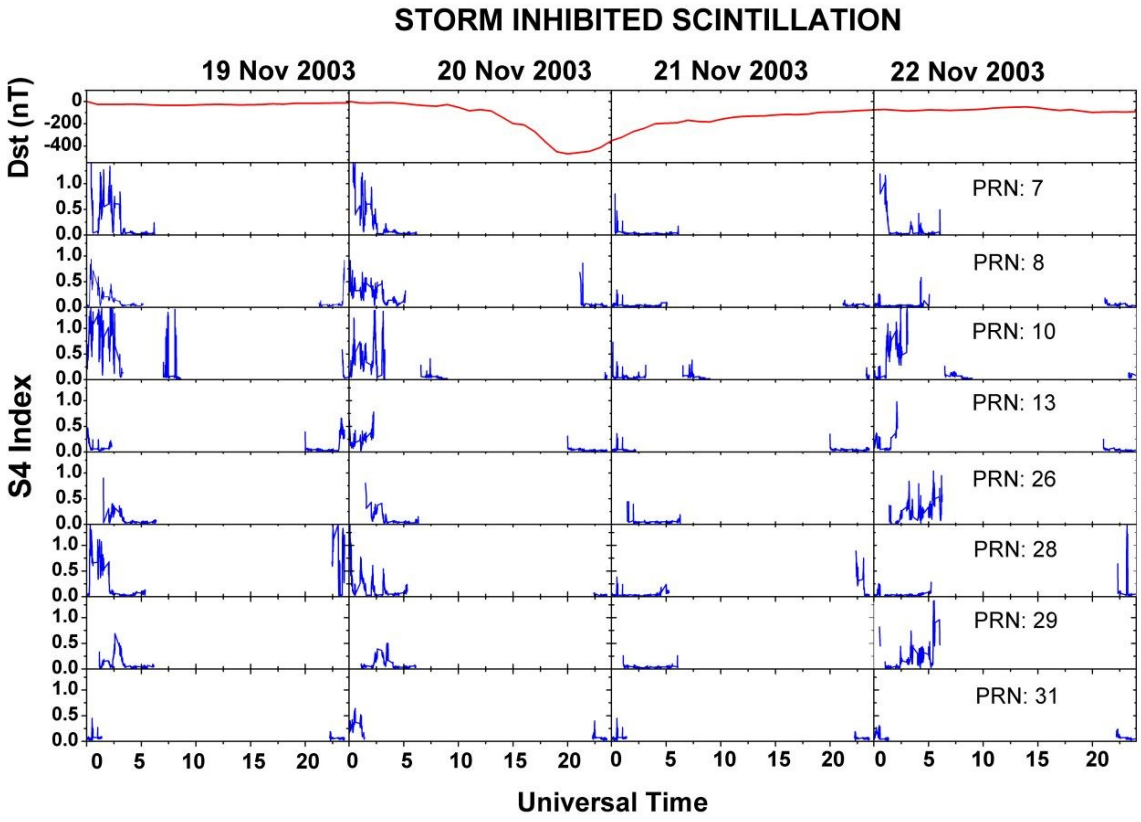

Figure 11: Example of scintillation inhibition during the night of 20/21 November 2003 few hours after the storm main phase. In the upper panel it is plotted the Dst index that reached almost -500 nT, which is considered a super strong storm (source: the authors).

During strong solar flare events, concurrent increases in the X-ray and EUV fluxes and solar radio bursts (SRB) can be observed. The SRBs cover a large range of frequencies including the L band, giving rise to signal fades in the GNSS C/No and fluctuations in its amplitude and phase (de Paula et al., 2022). The fades have larger amplitudes in the equator and decrease when latitude increases. The X-ray and the EUV intensified fluxes cause a sudden increase in the TEC. Gaps in the Digisonde signal can be observed due to increased D layer density caused by the short X-ray radiation intensification. All these effects are observed at receivers during sunlit hours and, even though they stay living for a short time, if they are strong, they also cause positioning errors in systems using the RTKlib. One example of GNSS fades during the X9.3 solar flare event that occurred on September 06, 2007, for the sites FRTZ (Fortaleza, 03.72°S, 38.54°W, dip latitude 09.43°S), INCO (Inconfidentes, 22.32°S, 46.33°W, dip latitude 20.33°S) and SJCU (São José dos Campos, 23.18°S, 45.89°W, dip latitude 21.22°S) is presented in Figure 13.

Augmentation systems were developed to comply with the FAA (Federal Aviation Administration) and ICAO (International Civil Aviation Organization) critical requirements for navigation and mainly for precision approach. These systems provide corrections and integrity for the GNSS measurements. One of these systems is the SBAS (Space- Based Augmentation System) where a network of ground reference GPS stations measures, among other corrections, the ionospheric corrections that are stored in a grid. Such corrections are transmitted to geostationary satellites that broadcast them to the GPS single frequency users. The other system is the GBAS (Ground Based Augmentation System) that is installed at airports that estimates code-pseudorange corrections based on multiple receiver on the ground (typically four) within the airport area and broadcast them to the aircrafts in the final phase of landing. The GBAS uses only the L1 band in the aircraft. These two systems have been successfully operational for the last decades at medium and high latitudes but they are vulnerable during the incidence of scintillations and strong ionospheric density gradients at low and equatorial regions, as reported in Lee et al. (2015), Yoon et al. (2020) and Affonso et al. (2022). DECEA (Department of Airspace Control) bought the GBAS station SLS-4000 from Honeywell in order to study its operational viability for Brazil and it was installed at Galeão airport, Rio de Janeiro. The equipment presented low performance in terms of availability during the scintillation events. Figure 14 shows the vertical accuracy for November 13, 2011 measured by a GPS receiver (magenta line) and by the GBAS station SLS-4000 (green dots) with its integrity monitors off. It is noticeable in Figure 14 that the vertical accuracy of GBAS has a degradation of its value in the hours between 23:00 and 1:00 UT. This period coincides with the time of occurrence of EPBs and consequently scintillation and strong spatio-temporal gradients of the TEC.

Even though threat models were developed to mitigate this problem in Brazil many operation restrictions imposed by this threat model limited the GBAS secure operations during some time windows and to restricted regional areas. These limitations of GBAS for the Brazilian regions are currently the subject of research by government institutions and universities.

Another ionospheric scintillation characteristic is that its behavior is different for different frequencies. Smaller scale size irregularities measured at L1 frequency (1.575 GHz) decay faster than larger scale size measured at UHF frequency (240 MHz). Figure 15 shows this behavior, where L1 scintillation (upper panel) disappears at 23:50 UT while scintillations are still observed from UHF (lower panel) from 24:30 to 25:00 UT. These data are from Ascension Island for March 27, 2000.

As previously mentioned, the bubbles are generated at the magnetic equator in the F region base and while uplifting they map to larger latitudes. After this growing phase, the bubbles move eastward with the ambient plasma and they decay after few hours due to recombination. During magnetic storms this eastward velocity normally turns to west. Using spaced GNSS or VHF receivers and the cross-correlation methodology, it is possible to calculate the zonal bubble drift, which is an important parameter to predict scintillation at sites located more to east, but it is a short-term prediction. Figure 16 presents the plasma irregularity zonal drift using spaced GPS receivers at Cachoeira Paulista for December 1998, and January and February 1999. It can be observed that this velocity is about 150 m/s at around 20:00 LT and it decreases as time passes by.

SCINTILLATION MITIGATION METHODOLOGIES

The use of GNSS technology for air navigation procedures has been a concern in low latitude regions due to the ionosphere, as analyzed for example in Rodrigues et al. (2022). Because of this and many other

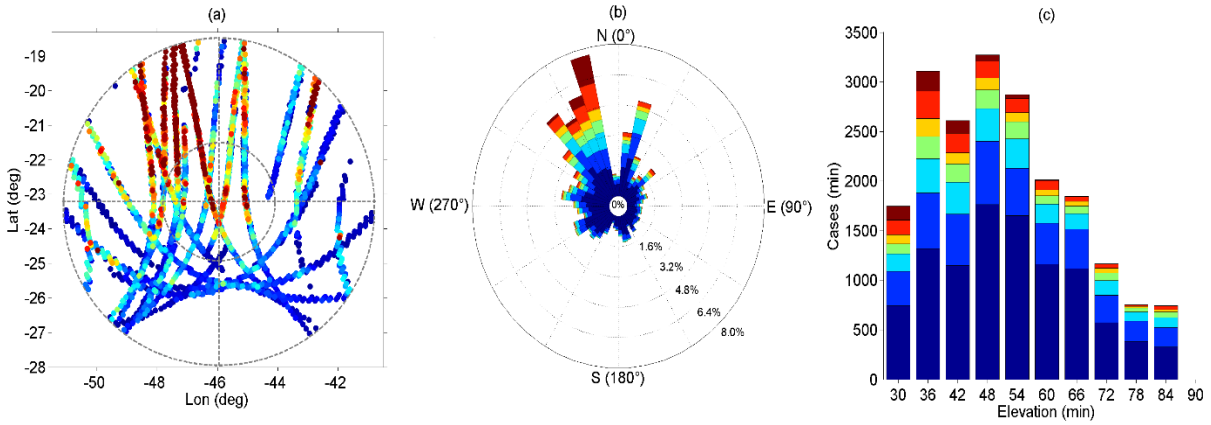

Figure 12: (a) The spatial distribution of amplitude scintillation events plotted at the respective IPP values for GPS-L1 signals. The outer and inner circles define elevations equal to 20° and 60°, respectively; (b) The statistical distribution of S_4 as a function of azimuth. The S_4 range groups for the azimuth and elevation plots share the same color code. (c) The statistical distribution of S_4 as a function of elevation is shown as bar charts (source: the authors).

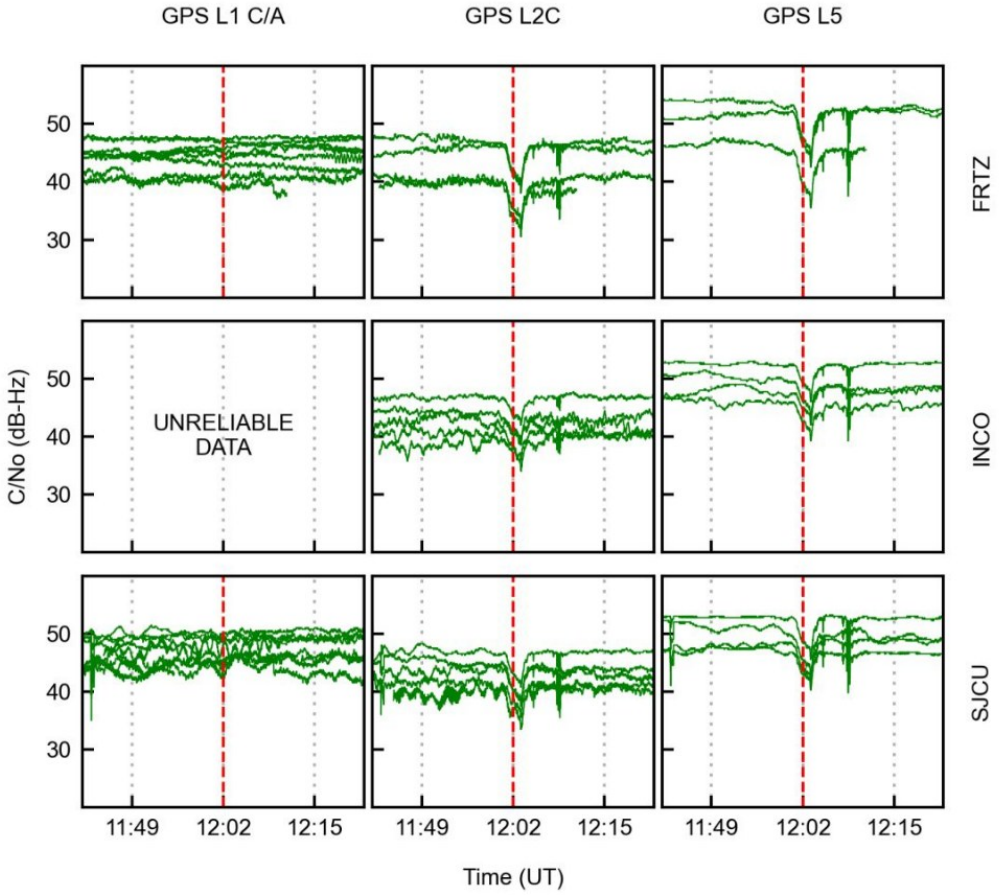

Figure 13: GPS C/No signal for L1, L2C and L5 GPS frequencies during 06 September 2017 for the sites FRTZ, INCO and SJCU. The vertical red line is the time of the solar flare maximum (source: de Paula et al., 2022).

applications, the necessity to mitigate ionospheric scintillation impacts on the GNSS positioning is a priority. Radio signals propagating through EPBs suffer C/N_0 degradation due to scintillation. Such an effect results in noisier pseudorange and carrier phase measurements, degrading positioning performance. In addition, availability problems can be caused by cycle slips and loss of lock in the receiver loops and these effects on simultaneously multiple links may even compromise navigation. Figure 17 shows a pictorial representation of an example application where GNSS channels from an aircraft are affected by scintillation.

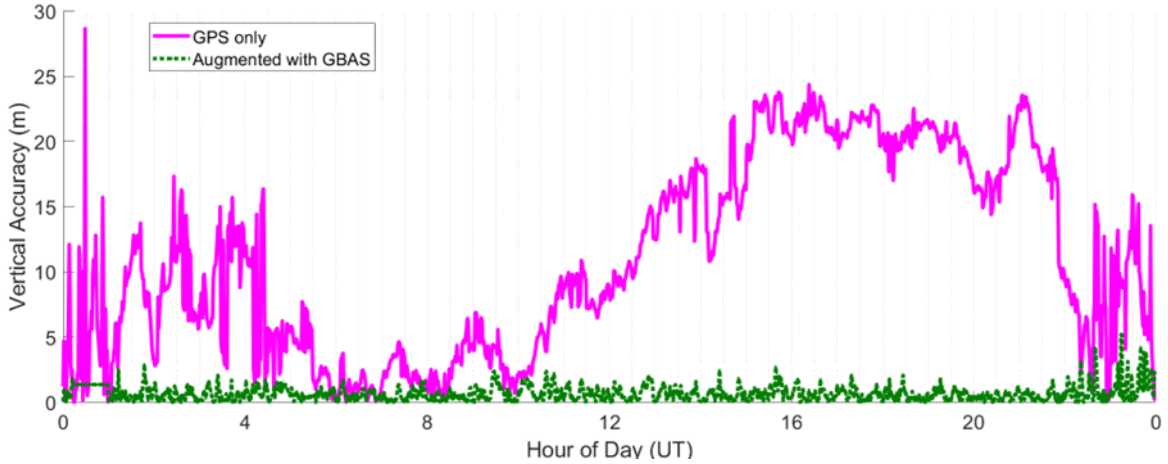

Figure 14: Vertical accuracy during field tests for GBAS Ground-Based Performance Monitor at Rio de Janeiro International Airport for November 13, 2011 (adapted from Marini-Pereira et al., 2019)

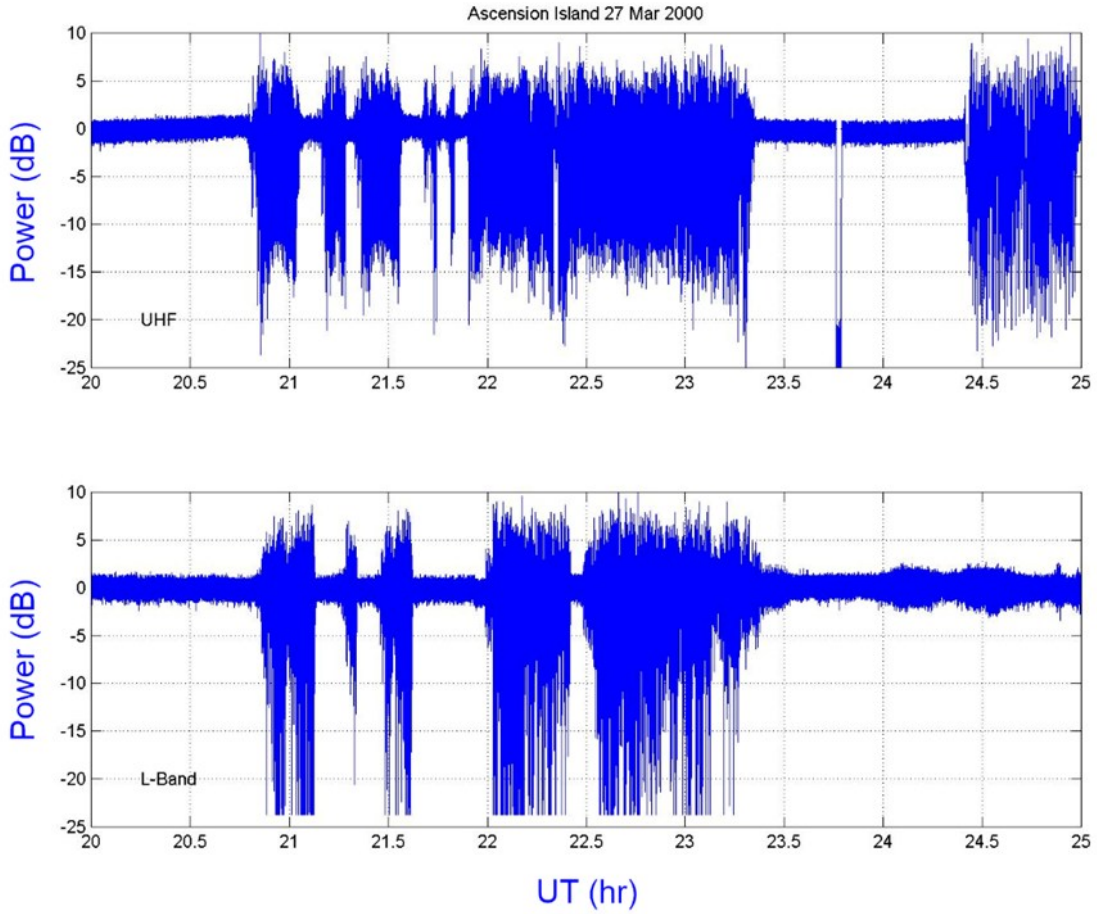

Figure 15: Simultaneous UHF (240 MHz) (upper panel) and L1 (1.575 GHz) (lower panel) from Ascension Island for March 27, 2000 (source: the authors).

In the upper right panel plot we can see the total number of GPS satellites being tracked and also the number of channels affected by scintillation during the night. In the lower panel we can see the positioning degradation in periods where the signals are affected by EPBs. This is one hypothetical example, but many other applications such as precision agriculture demand a more accurate positioning service. In many cases, as in this picture, for improving accuracy, it is common to use the concept of differential GPS, known in aviation as augmentation systems, which is an approach that broadcasts corrections to the users that have this demand. This context motivates research into

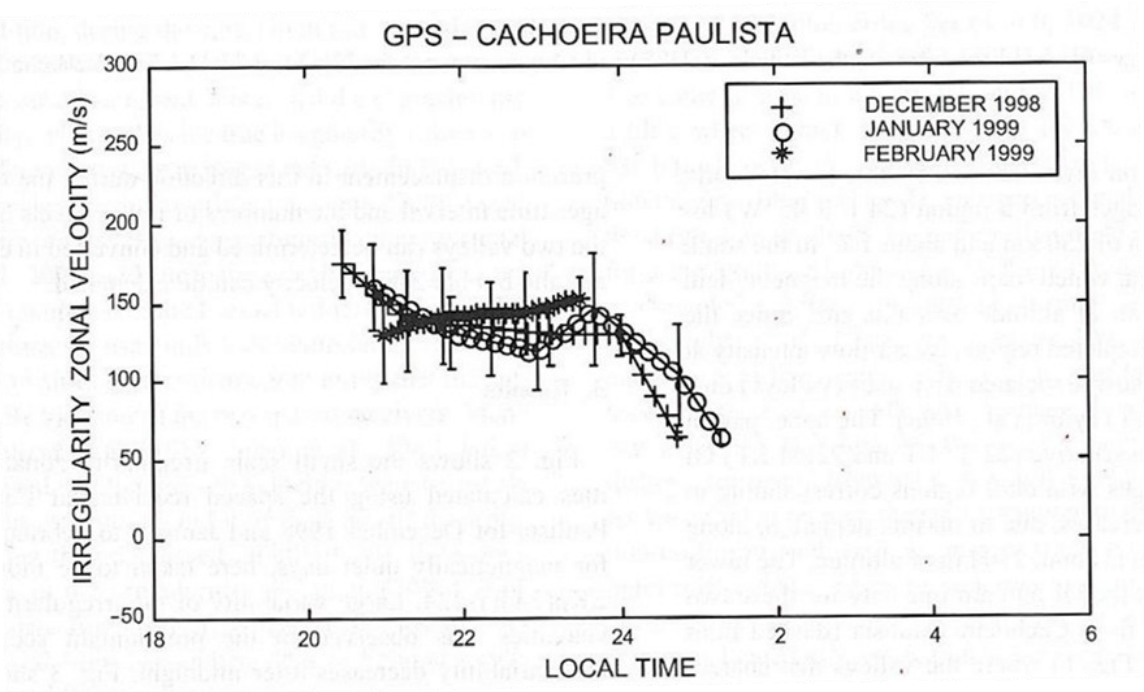

Figure 16: Plasma irregularity zonal drift using spaced GPS receivers at Cachoeira Paulista for December 1998, and January and February 1999 (source: de Paula et al., 2002).

techniques and methods to mitigate the effects of scintillation for GNSS users affected by EPBs.

One good contribution for improving the GNSS receiver capability for tracking signals even during the occurrence of scintillation was developed in the context of the projects CIGALA and CALIBRA. In these projects, some developments were carried out in order to try to improve the tracking capability of the receivers, as well as the mitigation strategy to reduce the effects of the scintillation. CIGALA and CALIBRA confirmed the vulnerability of GNSS high accuracy techniques to ionospheric disturbances, thorough a user performance review, where degradation in GNSS Precise Point Positioning (PPP) and Real Time Kinematic (RTK) positioning was seen to correlate with the occurrence of ionospheric scintillation and high TEC variability. This is especially so in Brazil due to its geographical location, extending across the magnetic equator, in one of the most troublesome ionospheric regions of the Earth, qualifying the country as a test-bed for worst case scenarios.

Concerning the mitigation, Aquino et al. (2009), using suitable receiver tracking models sensitive to ionospheric scintillation, that allow the computation of the variance of the output error of the receiver PLL (Phase Locked Loop) and DLL (Delay Locked Loop), expressing the quality of the range measurements used by the receiver to calculate user position, proposed a strategy using the Conker model (Conker, 2003) to obtain the covariance matrix of the observables. S_4 and sigmaPhi where the main parameters to be used in the stochastic model, for pseudorange and carrier phase, respectively. The results after applying such strategy showed improvement of the results of the order between 17 and 38% in height accuracy for an epoch-by-epoch differential solution over baselines ranging from 1 to 750 km.

More recently, in the context of the GNSS NavAer project (Monico et al., 2022), a new approach for ionospheric mitigation was proposed, based not only on the stochastic model, but also on the functional mode and a strategy to attenuate the effects of losses of lock and consequent ambiguity reinitializations that are caused by the need to reinitialize the tracking (Vani et al., 2019). An experiment using a 30-day static dataset affected by different levels of scintillation in the Brazilian southeastern region was used for testing the approach. Even with limitations imposed by data gaps, the results demonstrate improvements of up to 80% in the positioning accuracy. For the best cases, the approach can completely reduce the effects of ionosphere scintillation and recover the original PPP accuracy without any scintillation.

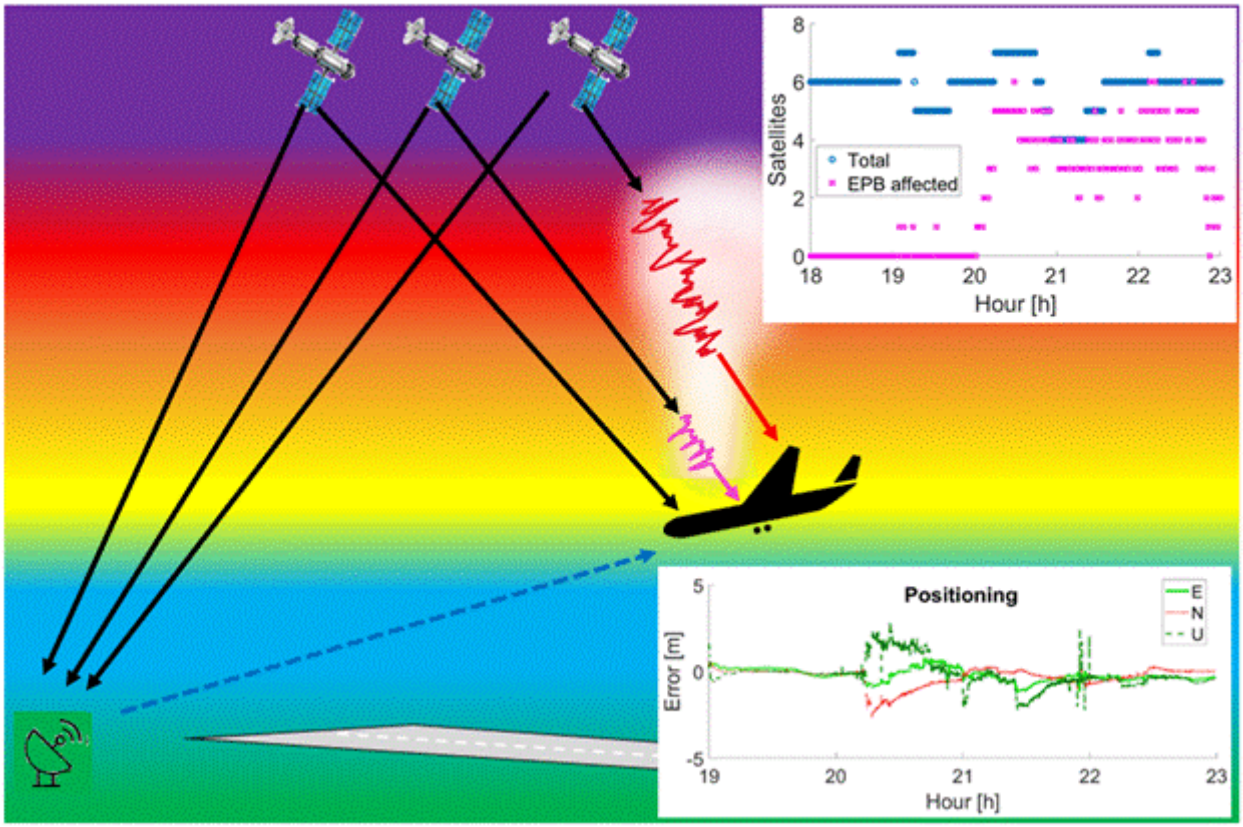

Figure 17: Pictorial example of an aircraft being affected by scintillation causing degradation in positioning accuracy (source: the authors).

Monico et al. (2017) proposed another approach, simpler than these ones. It was used just a data set that had S_4 larger than 0.9. The information from S_4 was added in the RTC Message for real time experiment. Only GPS and GLONASS satellites were available in the experiment. For one of the experiments, only few epochs with S_4 larger than 0.9 were available, while in the second, several values were available, mainly for GLONASS satellites. In the first experiment, considering the best solution, only in 6 epochs, out of 17288, the ambiguities could not be fixed. In the second one, when scintillation was stronger, it was 4834 epochs out of 13283 in the RTK solution. The carrier phase residuals were in the level of at maximum 0,5 cycle for the experiment #1, and more than one cycle for the other.

For GBAS mitigation:

1- The ionospheric threat model for Brazil to support GBAS was developed by an interagency team effort with contributions from Mirus Technology (an American company) funded by USTDA, the FAA, the DECEA, Stanford University, Boston College, Kaist, ICEA, and INPE (Lee et al., 2017; Yoon et al., 2017). This concept of the model was similar to the standard ionospheric threat model used initially in CONUS, but using GNSS data from Brazil during the peak of solar cycle 23;

2- Pereira (2018) also computed ionospheric gradients over the Brazilian territory aiming at generating an independent ionospheric threat model to support GBAS in Brazil. Since the values found for ionosphere gradients far exceeded the limits used in CONUS, for any elevation value of the satellites, its use in the approach of the Position Domain Geometry Screening (Lee et al., 2011) would severely decrease the system's availability, as demonstrated by Yoon et al. (2016). The largest gradients were obtained during the autumn, spring, and summer, for the period from 22:00 to 5:00 TU and for the regions of geomagnetic latitudes between 10° and 20° and between -40° and -10°, as well as longitudes between -60° and -35°. On the other hand, during the winter period, and excluding satellites with elevations between 10° and 30°, the gradients were below the CONUS threat model limits;

3- A new GBAS methodology with Multi-Constellations (MC Multi- (MF) was recently proposed according to Caamano et al. (2016);

4- In Marini-Pereira et al. (2022), it was proposed a strategy to enhance the performance of GBAS under low-latitude ionospheric environments. This method consisted of a detection and warning system based on a cluster of ground ionospheric monitoring stations around the GBAS facility area (typically within a radius of 10 km). This system was designed to work in real-time, detecting and alerting scenarios where availability and integrity threats have the potential to happen. The system monitoring criterion is based on time-step gradients in the ionospheric delay, which are used as a test statistic together with data gap analysis. Experimental results showed that the method is quite effective in detecting threatening gradients.

CONCLUSIONS

This work revisits the characteristics of plasma irregularities that cause scintillation in the GNSS and then describes their effects on the GNSS signals and positioning systems, as well as over the augmentation systems like the SBAS and GBAS. Methodologies to mitigate these effects are also presented. The main highlights are:

- the plasma irregularities that cause scintillation in the GNSS signal present a large day-to-day variability (Abdu, 2019) and the most common indexes to study scintillation are the S_4 and the σ_φ representing the amplitude and phase scintillations respectively;
- to better characterize the amplitude scintillation severity, it is recommended to calculate the decorrelation time parameter τ_0 besides analyzing the S_4 index;
- loss of lock, GDOP increase and decrease of number of available satellites are critical situations caused by strong scintillation that can deteriorate or even hinder the GNSS operation;
- the new civil signals L2C and L5 are more susceptible to the effects of the ionospheric scintillation in low latitudes;
- the scintillation occurrence at low latitude initiates around 19:30 LT and lasts up to 01:30 LT during high solar activity and this time interval decreases during low solar activity. The scintillation intensity and percentage of occurrence are higher for higher solar flux;
- bubbles at Brazilian low latitude start in September and extend up to March/April, having maximum occurrence during summer solstice (November –January). The alignment between the magnetic field lines and the terminator line (day-night), besides the vertical plasma drift at the magnetic equator (Fejer et al., 1999), is an important factor that determines the seasonality and the occurrence or not of the irregularities at determined site;
- S_4 amplitude depends of the ionospheric background ionization and due to the EIA it increases from magnetic equator ($S_4 \leq 0.30$) to the EIA crest, where S_4 can reach amplitude as large as 1.40;
- the SF (Spread F) occurrence is much larger at Cachoeira Paulista (magnetic declination 21° W) than at Tucumán (magnetic declination 3 °) in the north of Argentina. Tucumán is westward of Cachoeira Paulista but even having almost the same dip latitude of Cachoeira Paulista it presents much less scintillation occurrence, showing a large longitudinal effect;
- the magnetic storms have substantial effects over the scintillation. If there is prompt penetration of equatorial eastward electric field (PPEF) from magnetosphere into equatorial region during the prereversal hours, the upward drift is intensified and plasma irregularities can be generated even during no scintillation season. On the other hand, the DDEF, that is generated due to the disturbed thermospheric wind caused by storm heating at auroral regions, is westward during daytime and prereversal hours. This DDEF inhibits the prereversal plasma drift peak and consequently the generation of plasma irregularities. It takes some hours after the storm main phase for this process to set up one westward electric field at the magnetic equator;
- the alignment between the GNSS signal and the magnetic field lines, when the signals are more likely to propagate a longer distance in the turbulent medium created by the bubbles, gives origin to interruptions due to the loss of phase lock, since there are large amplitude fades (canonical) and increased phase scintillations;

- during strong solar flare events, concurrent increases in the X-ray and EUV fluxes and SRB can be observed. The SRBs cover a large range of frequencies including the L band, giving rise to signal fades in the GNSS C/No and fluctuations in its amplitude and phase that can cause positioning errors in systems using the RTKlib;
- the augmentation systems SBAS and GBAS have been successfully operational for the last decades at medium and high latitudes but they fail during the incidence of scintillations and large ionospheric density gradients at low and equatorial regions;
- the ionospheric scintillation behavior is different for different frequencies. For instance, smaller scale size irregularities in the L1 frequency (1.575 GHz) decay faster than larger scale size scintillations in the UHF frequency of 240 MHz;
- the ionospheric bubbles, after the growing phase, normally drift to east with an approximate velocity of 150 m/s around 20 LT and this velocity decays along the night up to the bubble extinction few hours later due to collisions. During a magnetic storm, this eastward velocity normally turns to west;
- good contributions for improving the GNSS receiver capability for tracking signals even during the occurrence of scintillation were developed in the context of the projects CIGALA and CALIBRA;
- new approaches for ionospheric mitigation were successfully proposed, based not only on the stochastic model, but also on the functional mode and a strategy to attenuate the effects of losses of lock and consequent ambiguity reinitializations that are caused by the need to reinitialize the tracking;
- for GBAS mitigation, ionospheric threat models for Brazil were developed; however, due to many restrictions imposed by these models, the GBAS was not implemented by DECEA. Additionally, new GBAS methodologies based on MC and MF were recently proposed and are in the development phase.

ACKNOWLEDGMENTS

This work has been performed in the framework of the INCT GNSS-NavAer Project under grants CNPq 465648/2014-2 and FAPESP 2017/50115-0. ERP thanks Brazilian Ministry of Science, Technology and Innovation, Brazilian Space Agency and CNPq 202531/2019-0. AM and JFGM are grateful respectively to CNPq 309389/2021-6 and 304773/2021-2.

REFERENCES

Abdu, M.A., 2019, Day-to-day and short-term variabilities in the equatorial plasma bubble/spread F irregularity seeding and development: Prog. Earth Planet Sci., **6**, 11, doi: 10.1186/s40645-019-0258-1.

Abdu, M.A., J.H.A. Sobral, I.S. Batista, V.H. Rios, and C. Medina, 1998, Equatorial spread-F occurrence statistics in the American longitudes: diurnal, seasonal and solar cycle variations: Adv. Space Res., **22**, 6, 851–854, doi: 10.1016/S0273-1177(98)00111-2.

Abdu, M. A., J. R. de Souza, E. A. Kherani, I. S. Batista, J. W. MacDougall, and J. H. A. Sobral, 2015, Wave structure and polarization electric field development in the bottomside *F* layer leading to postsunset equatorial spread *F*: J. Geophys. Res. Space Physics, **120**, 6930–6940, doi: 10.1002/2015JA021235.

Affonso, B.J., A. Moraes, J. Sousasantos, L. Marini-Pereira, and S. Pullen, 2022, Strong ionospheric spatial gradient events induced by signal propagation paths aligned with equatorial plasma bubbles: IEEE Transactions on Aerospace and Electronic Systems, **58**, 4, 2868–2879, doi: 10.1109/TAES.2022.3144622.

Aquino, M., J.F.G. Monico, A.H. Dodson, H.A. Marques, G. de Franceschi, L. Alfonsi, V. Romano, and M. Andreotti, 2009, Improving the GNSS positioning stochastic model in the presence of ionospheric scintillation: J. Geod., **83**, 953–966, 10.1007/s00190-009-0313-6

Caamano, M., M. Felux, M.-S. Circiu, and D. Gerbeth, 2016, Multi-constellation GBAS: how to benefit from a second constellation: 2016 IEEE/ION Position, Location and Navigation Symposium (PLANS), Savannah, GA, USA, 833–841, doi: 10.1109/PLANS.2016.7479779.

Carrano, C. S., and K. M. Groves, 2010, Temporal decorrelation of GPS satellite signals due to multiple scattering from ionospheric irregularities: Proceedings of the 23rd International Technical Meeting of the Satellite Division of the Institute of Navigation (ION GNSS 2010), Portland, OR, USA, 361–374.

Conker, R. S., El-Arini, M. B., Hegarty, C. J. and Hsiao, T., 2003, Modeling the effects of ionospheric scintillation on GPS/Satellite-Based Augmentation System availability: Radio Science, **38**, ISSN: 0048-

6604, doi: 10.1029/2000RS002604.

de Oliveira, C. B. A., Espejo, T. M. S., Moraes, A., Costa, E., Sousasantos, J., Lourenço, L. F. D. and Abdu, M. A., 2020, Analysis of Plasma Bubble Signatures in Total Electron Content Maps of the Low-Latitude Ionosphere: A Simplified Methodology: Surveys in Geophysics, **41**, 4, 897–931, doi: 10.1007/s10712-020-09584-7.

de Paula, E. R., and D. L. Hysell, 2004, The São Luís 30 MHz coherent scatter ionospheric radar: system description and initial results: Radio Sci., **39**, RS1014, doi: 10.1029/2003RS002914.

de Paula, E.R., Kantor, I.J., Sobral, J.H.A., Takahashi, H., Santana, D.C., Gobbi, D., de Medeiros, A.F., Limiro, L.A.T., Kil, H., Kintner, P.M. and Taylor, M.J., 2002, Ionospheric irregularity zonal velocities over Cachoeira Paulista: Journal of Atmospheric and Solar-Terrestrial Physics, **64**, 1511–1516, doi: 10.1016/S1364-6826(02)00088-3.

de Paula, E. R., Oliveira, C. B. A., Caton, R. G., Negreti, P. M. S., Batista, I. S., Martinon, A. R. F., Neto, A. C., Abdu, M. A., Monico, J. F. G., de Souza, J. R., and Moraes, A. O., 2019, Ionospheric irregularity behavior during the September 6-10, 2017 magnetic storm over Brazilian equatorial-low latitudes, Earth, Plan. and Space, **71**, 42, doi: 10.1186/s40623-019-1020-z.

de Paula, E. R., Moraes, A. O., Abdu, M. A. , Sobral, J. H. A., Batista, I. S., Kherani, E. A., Takahashi, H. and Costa, E., 2021a, Long Term Studies on Ionospheric Scintillation and Plasma Bubbles, 100 Years of the International Union of Radio Science, Eds. P. Wilkinson, P. S. Cannon and W. R. Stone, URSI Press, Gent, Belgium, ISBN 9789463968034.

de Paula, E. R., Martinon, A. R. F., Moraes, A. O., Carrano, C., Neto, A. C., Doherty, P., Groves , K., Valladares, C. E., Crowley, G., Azeem, I., Reynolds, A., Akos, D. M., Walter, T., Beach, T. L. and Slewaegen, J.-M., 2021b, Performance of 6 different global navigation satellite system receivers at low latitude under moderate and strong scintillation: Earth and Space Science, **8**, e2020EA001314, 10.1029/2020EA001314.

de Paula, E. R., Martinon, A.R. F., Carrano, C., Moraes, A. O., Neri, J. A. C. F., Cecatto, J. R., Abdu, M. A., Neto, A. C., Monico, J. F. G., Silva, W. C., Vani, B. C., Batista, I. S., Mendes, O., De Souza, J. R. and Silva, A. L. A., 2022, Solar flare and radio burst effects on GNSS signals and the ionosphere during September 2017: Radio Science, **57**, e2021RS007418, doi: 10.1029/2021RS007418.

de Paula, E. R., Monico, J. F. G., Tsuchiya, I. H., Valladares, C. E., Costa, S. M. A., Marini-Pereira, L., Vani, B. C., and Moraes, A. O., 2023, A retrospective of Global Navigation Satellite System ionospheric irregularities monitoring networks in Brazil: Journal of Aerospace Technology and Management, **15**, e0123, doi: 10.1590/jatm.v15.1288.

Doherty, P. H., Delay, S. H., Valladares, C. E. and Klobuchar, J. A., 2003, Ionospheric scintillation effects on GPS in the equatorial and auroral regions: J. Inst. Navig., **50**, 4, 235–246, doi: 10.1002/j.2161-4296.2003.tb00332.x.

Fejer, B. G., Scherliess, L., de Paula, E. R., 1999, Effects of the vertical plasma drift velocity on the generation and evolution of equatorial spread *F*: J. Geophys. Res., **104**, 19859–19869, doi: 10.1029/1999JA900271.

Kintner, P. M., Kil, H., Beach, T. L. and de Paula, E. R., 2001, Fading timescales associated with GPS signals and potential consequences: Radio Science, **36**, 4, 731–743, doi: 10.1029/1999RS002310

Lee, J., Seo, J., Park, Y. S., Pullen, S. and Enge, P., 2011, Ionospheric threat mitigation by geometry screening in ground-based augmentation systems: Journal of Aircraft, **48**, 4, 1422–1433, doi: 10.2514/1.C031309.

Lee, J., Yoon, M., Pullen, S., Gillespie, J., Mather, N., Cole, R. and Pradipta, R., 2015, Preliminary results from ionospheric threat model development to support GBAS operations in the Brazilian region: Proceedings of the 28th International Technical Meeting of The Satellite Division of the Institute of Navigation (ION GNSS+ 2015), pp. 1500–1506.

Lee, Jiyun, Morton, Y, Lee, J., Moon H.-S., Seo, J., 2017, Monitoring and Mitigation of Ionospheric Anomalies for GNSS-Based Safety Critical Systems: A review of up-to-date signal processing techniques: IEEE Signal Processing Magazine, **34**, 5, 96–110, doi: 10.1109/MSP.2017.2716406.

Marini-Pereira, L., de Oliveira, K., Salles, L. A., Moraes, A. D. O., de Paula, E. R., Muella, M. T. D. A. H. and Perrella, W. J., 2019, On the field validation of α-μ fading coefficients estimator based on the autocorrelation function for ionospheric amplitude scintillation: Advances in Space Research, **64**, 10, 2176–2187, doi: 10.1016/j.asr.2019.06.012.

Marini-Pereira, L., Pullen, S., Moraes, A. O. and Sousasantos, J., 2021, Ground-based augmentation systems operation in low latitudes - Part 1: Challenges, mitigations, and future prospects: Journal of Aerospace Technology and Management, **13**, e4621, doi: 10.1590/jatm.v13.1236.

Marini-Pereira, L., Moraes, A. O. and Pullen, S., 2022, Advanced Warning of Threatening Equatorial Plasma Bubbles to Support GBAS in Low Latitudes: IEEE Transactions on Aerospace and Electronic Systems, 2023.

Misra, P., and Enge, P., 2006, Global positioning system: Signals, Measurements and Performance, *in* Global Positioning System: Signals, Measurements and Performance, Lincoln, MA,

Ganga-Jamuna Press, pp: 381–384.

Monico, J.F.G., Tsuchiya, I. and Fiorini, F., 2017, Results on Ionospheric Scintillation Mitigation Using GPS and GLONASS: AGU Fall Meeting, New Orleans, LA, USA.

Monico, J. F. G., Paula, E. R. D., Moraes, A. O., Costa, E., Shimabukuro, M. H., Alves, D. B. M. and Aguiar, C. R., 2022, The GNSS NavAer INCT Project Overview and Main Results: Journal of Aerospace Technology and Management, 14, e0722, doi: 10.1590/jatm.v14.1249.

Moraes, A.O., Rodrigues, F. S., Perrella, W. J. and de Paula, E. R., 2011, Analysis of the Characteristics of Low-Latitude GPS Amplitude Scintillation Measured During Solar Maximum Conditions and Implications for Receiver Performance, Surveys in Geophysics, **33**, 5, 1107–1131, doi: 10.1007/s10712-011-9161-z.

Moraes, A. O., de Paula, E. R., Muella, M. T. D. A. H. and Perrella, W. J., 2014, On the second order statistics for GPS ionospheric scintillation modeling, Radio Science, **49**, 2, 94–105, doi: 10.1002/2013RS005270.

Moraes, A. O., Costa, E., Abdu, M. A., Rodrigues, F. S., de Paula, E. R., Oliveira, K. and Perrella, W. J., 2017, The variability of low-latitude ionospheric amplitude and phase scintillation detected by a triple-frequency GPS receiver: Radio Sci., **52**, 439–460, doi: 10.1002/2016RS006165.

Moraes, A. D. O., Vani, B. C., Costa, E., Sousasantos, J., Abdu, M. A., Rodrigues, F. and Monico, J. F. G., 2018a, Ionospheric scintillation fading coefficients for the GPS L1, L2, and L5 frequencies: Radio Science, **53**, 9, 1165–1174, doi: 10.1029/2018RS006653.

Moraes, A. D. O., Vani, B. C., Costa, E., Abdu, M. A., de Paula, E. R., Sousasantos, J. Monico, J. F. G., Forte, B., Negreti, P. M. S. and Shimabukuro, M. H., 2018b, GPS availability and positioning issues when the signal paths are aligned with ionospheric plasma bubbles: GPS Solutions, **22**, 4, 95, doi: 10.1007/s10291-018-0760-8.

Moraes, A., Sousasantos, J., de Paula, E. R., da Cunha, J. J. P. P., Lima Filho, V. C. and Vani, B. C., 2019, Performance analysis of κ-μ distribution for Global Positioning System (GPS) L1 frequency-related ionospheric fading channels: Journal of Space Weather and Space Climate, **9**, A15, doi: 10.1051/swsc/2019012.

Moraes, A., J. Sousasantos, B. J. Affonso, P. R. P. Silva, E. R. De Paula and J. F. G. Monico, 2023, Statistical Evaluation of the Role of GNSS Signal Propagation Orientation in Low-latitude Amplitude Scintillation Severity. IEEE Open Journal of Antennas and Propagation, **4**, 602–613, 2023, doi: 10.1109/OJAP.2023.3290981.

Muella, M. T. A. H., Kherani, E. A., de Paula, E. R., Cerruti, A. P., Kintner, P. M., Kantor, I. J., Mitchell, C. N., Batista, I. S. and Abdu, M. A., 2010, Scintillation-producing Fresnel-scale irregularities associated with the regions of steepest TEC gradients adjacent to the equatorial ionization anomaly: J. Geophys. Res., **115**, A03301, https://doi.org/10.1029/2009JA014788

Muella, M. T., Duarte-Silva, M. H., Moraes, A. O., de Paula, E. R., de Rezende, L. F., Alfonsi, L. and Affonso, B. J., 2017, Climatology and modeling of ionospheric scintillations and irregularity zonal drifts at the equatorial anomaly crest region: Annales Geophysicae, **35**, 6, doi: 10.5194/angeo-35-1201-2017

Pereira, V. A. S., 2018, Investigação da usabilidade do GBAS no Brasil: PhD. Thesis. Universidade Estadual Paulista (Unesp), Presidente Prudente, SP, Brazil. 305 pp.

Portella, I. P., Moraes, A., O., da Silva Pinho, M., Sousasantos, J. and Rodrigues, F., 2021, Examining the tolerance of GNSS receiver phase tracking loop under the effects of severe ionospheric scintillation conditions based on its bandwidth: Radio Science, **56**, 6, e2020RS007160, doi: 10.1029/2020RS007160.

Rodrigues, R. G., Fulindi, J. B., Oliveira, D. B. P. D., Moraes, A. D. O., and Marini-Pereira, L., 2022, Safety Analysis of GNSS Parallel Runway Approach Operation at Guarulhos International Airport: Journal of Aerospace Technology and Management, 14, e1622, doi: 10.1590/jatm.v14.1260.

Salles, L. A., Moraes, A., Vani, B., Sousasantos, J., Affonso, B. J. and Monico, J. F. G., 2021a, A deep fading assessment of the modernized *L2C* and *L5* signals for low-latitude regions: GPS Solutions, 25, 3, 122, 1–13, doi: 10.1007/s10291-021-01157-4.

Salles, L. A., Vani, B. C., Moraes, A., Costa, E., de Paula, E. R., 2021b, Investigating ionospheric scintillation effects on multifrequency GPS signals: Surveys in Geophysics, **42**, 4, 9991025, doi: 10.1007/s10712-021-09643-7.

Sato, H., Kim, J. S., Otsuka, Y., Wrasse, C. M., de Paula, E. R. and de Souza, J. R., 2021, L-band Synthetic Aperture Radar observation of ionospheric density irregularities at equatorial plasma depletion region: Geophysical Research Letters, **48**, https://doi.org/10.1029/2021GL093541

Sobral, J. H. A., Abdu, M. A., Takahashi, H., Taylor, M. J., de Paula, E. R., Zamlutti, C. J., de Aquino, M. G. and Borba, G.L., 2002, Ionospheric plasma bubble climatology over Brazil based on 22 years (1977–1998) of 630 nm airglow observations: J. Atmos. Solar Terr. Phys., **64**, 12–14, 1517–1524, doi: 10.1016/S1364-6826(02)00089-5.

Souza, A. L. C. D., Jerez, G. O., Camargo, P. D. O and Alves, D. B. M., 2022, Assessment of GPS positioning performance using different signals in

the context of ionospheric scintillation: a month-long case study on São José dos Campos, Brazil: Boletim de Ciências Geodésicas, **28**, 4, e2022018, doi: 10.1590/s1982-21702022000400018.

Sousasantos J., Marini-Pereira, L., Moraes, A. O. and Pullen, S., 2021, Ground-Based Augmentation System Operation in Low Latitudes - Part 2: Space Weather, Ionospheric Behavior and Challenges: Journal of Aerospace Technology and Management, **13**, doi: 10.1590/jatm.v13.1237.

Sousasantos, J., Affonso, B. J., Moraes, A., Rodrigues, F. S., Abdu, M. A.,Salles, L. A. and Vani, B. C., 2022, Amplitude scintillation severity and fading profiles under alignment between GPS propagation paths and equatorial plasma bubbles: Space Weather, **20**, e2022SW003243, doi: 10.1029/2022SW003243.

Takahashi, H., Wrasse, C. M., Denardini, C. M., Pádua, M. B., de Paula, E. R., Costa, S. M. A., Otsuka, Y., Shiokawa, K., Galera Monico, J. F., Ivo, A. and Sant'Anna, N., 2016, Ionospheric TEC Weather Map Over South America: Space Weather, **14**, 937–949, doi: 10.1002/2016SW001474.

Van Dierendonck, A. J., Klobuchar J. and Hua, Q., 1993, Ionospheric Scintillation Monitoring Using Commercial Single Frequency C/A Code Receivers, Proceedings of ION GPS-93, Salt Lake City, UT, September.

Vani, B. C., Forte, B., Monico, J. F. G., Skone, S., Shimabukuro, M. H., Moraes, A. O., Portella, I. P. and Marques, H. A., 2019, A Novel Approach to Improve GNSS Precise Point Positioning During Strong Ionospheric Scintillation: Theory and Demonstration, IEEE Transactions on Vehicular Technology, **68**, 5, 4391–4403, doi: 10.1109/TVT.2019.2903988.

Yokoyama, T., 2017, A review on the numerical simulation of equatorial plasma bubbles toward scintillation evaluation and forecasting: Prog. Earth Planet. Sci, **4,** 37, doi: 10.1186/s40645-017-0153-6.

Yoon, M., Kim, D., Lee, J., Rungruengwajiake, S. and Pullen, S., 2016, Assessment of equatorial plasma bubble impacts on Ground-Based Augmentation Systems in the Brazilian region: Proceedings of the 2016 International Technical Meeting of The Institute of Navigation, Monterey, California, 368–379, doi: 10.33012/2016.13423.

Yoon, M., Lee, J., Pullen, S., Gillespie, J., Mathur, N., Cole, R., De Souza, J.R., Doherty, P. and Pradipta, R., 2017, Equatorial plasma bubble threat parameterization to support GBAS operations in the Brazilian region, Navigation: Journal of The Institute of Navigation, **64**, 3, 309–321, doi: 10.1002/navi.203.

Yoon, M., Kim, D. and Lee, J., 2020, Extreme ionospheric spatial decorrelation observed during the March 1, 2014, equatorial plasma bubble event: GPS Solutions, **24**, 2, 1–11, doi: 10.1007/s10291-020-0960-x.

Paula, E.R.: idea development, writing – original draft, validation of methods and investigations, validation of the most relevant results presented regarding scintillation characteristics and their effects on GNSS signals and position/navigation systems in the Brazilian region, discussion, revision, manuscript final version contribution; **Moraes, A.O.**: validation of methods and investigations, validation of the most relevant results presented regarding scintillation characteristics and their effects on GNSS signals and position/navigation systems in the Brazilian region, discussion, revision, manuscript final version contribution; **Monico, J.F.G.**: validation of methods and investigations, validation of the most relevant results presented regarding scintillation characteristics and their effects on GNSS signals and position / navigation systems in the Brazilian region, discussion, revision, manuscript final version contribution.

Received on August 12, 2022 / Accepted on October 19, 2022